

Morphology of Segmented Polyether Based Poly(urea-urethane) Thermoplastic Elastomers

Jia-Yi LIU,¹ Yueh-Chin HSU,² and Yen-Zen WANG^{1,†}

¹Graduate School of Engineering Science and Technology (Doctoral program),
National Yunlin University of Science and Technology, Yunlin, Taiwan 640

²General Education Division, Nan-Jeon Institute of Technology, Taiwan, Taiwan 737

(Received January 10, 2006; Accepted May 18, 2006; Published July 24, 2006)

ABSTRACT: New aniline-containing segmented poly(urea-urethane) (PUU-OPA) based on polyether polyurethane prepolymer and an oligomer of amine-terminated polyaniline (OPA) were prepared as a conductive material. The amine-terminated functional groups of OPA were introduced into the poly(urea-urethane) (PUU) structure as a chain extender to form the hard segment of the copolymer with urea-linkage. The morphology of PUU-OPA was examined by the transmission electron microscopy (TEM) and solid-state ¹³C NMR approaches. The conductivity of the copolymers is found to be ranged from 0.83 S/cm for the neat OPA to 1.96×10^{-6} S/cm for the resultant copolymers. TEM measurements clearly reveal the microphase separation. Various contact time CP experiments indicate that T_{CH} and $T_{1\rho}(H)$ of the soft segment carbons declined as the OPA content increased. These results indicate that the chain mobility and the domain size of the soft segment in the copolymer on the nanophase scale gradually decreased as the OPA content increased. [doi:10.1295/polymj.PJ2005204]

KEY WORDS ¹³C NMR / TEM / Poly(urea-urethane) / Morphology / Polyurethane /

Polyaniline (PANI), one of the most promising intrinsically conducting polymers, has been attracted considerable attention in recent years because it has a relatively high conductivity and potential application in electronic devices.^{1,2} Polyaniline is generally prepared by oxidative the polymerization of aniline in acid media using an external oxidant such as ammonium peroxydisulfate, $(NH_4)_2S_2O_8$, and can exist as a number of unique structures, characterized by the oxidation state, which determines the ratio of amine to imine nitrogens, and the extent of protonation.³ The emeraldine base (EB) is one of the several possible structures. The conducting form of polyaniline can be easily prepared by doping the EB with a protonic acid resulting in a complex acid salt. The members of the polyaniline family are difficult to handle because of their brittleness and poor solubility in polar organic solvents. The processing of emeraldine base is difficult, because EB decomposes below its softening or melting temperature.^{4–7} Therefore, the processibility of EB has been the subject of several investigations over the last few years.^{8–11} The earlier attempts at processing polyaniline focused on modifying the chain structure by copolymerization or derivation with hydrophilic or alkyl groups. These attempts resulted in a first successful step toward the so-called soluble polymer. Recently, attempts have been made to synthesize aniline oligomers with well-defined structures and amine end-groups and thus improve their solubility and capacity to undergo further poly-

merization have been reported.^{12–18} Polyurethanes (PU), comprising a polyether or polyester soft (flexible) segment and a diisocyanate-based hard (rigid) segment, are well known to be tough materials and are typically employed as additives to improve the toughness of brittle materials. The incompatibility between the hard segment and the soft segment causes polyurethanes undergo to microphase separation resulting in a hard-segment domain, soft-segment matrix, and urethane-bonded interphase. The hard-segment domains act as physical cross-links in the soft-segment matrix. Physical crosslinking of thermoplastic elastomers occurs by affinity of the hard segments as a result of their microheterogenous, two-phase morphology. The rigidity of polyurethane blocks is due to the 1-D ordering and hydrogen-bonding between hard segments. The hard domains comprise a minor, discontinuous phase dispersed in the major, continuous phase composed of the rubber blocks from different copolymer chains. The hard domains as physical crosslinks to hold together the soft, rubber domains. The primary driving force of microphase separation is the strong intermolecular interaction among the urethane units, which can form inter-urethane hydrogen bonds. In most investigations, the degree of microphase separation has been found to be incomplete. That is, microdomains are not pure as a result of inter-segmental mixing. Mixing within the soft microphase is reflected by an elevation in its glass transition temperature as compared to the pure component.¹⁹ The

[†]To whom correspondence should be addressed (Tel: +886-5-5342601 ext 4617, Fax: +886-5-5312071, E-mail: wangzen@yuntech.edu.tw).

degree of miscibility of hard segments within the soft microphase is associated with the broad distribution of hard segment sequence lengths. Shorter hard segments might be expected to remain within the soft microphase. The evaluation of the fraction of hard segments mixing within the soft microphase has been estimated by Koberstein *et al.*²⁰ For some time now, the physical properties of conductive polymers have been known to be significantly altered by chemical modification using appropriate non-conducting host polymers. Copolymerization is a significant approach of improvement. Researchers have synthesized various copolymers of polyaniline, including the poly(aniline-*co*-toluidine).^{21–25} Our previous investigation reported the chemical method, involving the copolymerization of a urethane block and an aniline-containing urethane-urea block, to improve processibility and mechanical properties.²⁶ The questions to be further answered concerning such block copolymers are whether the microstructure can be formed and how the mixed phase can be influenced by the molecular architecture and chemical composition can affect the mixed phase.

Various approaches such as transmission electron microscopy (TEM), and light scattering and neutron scattering and reflectivity have been employed to characterize and analyzing the microphase structure of a particular block copolymer system.^{27–29} Probably one of the most powerful tools available for providing insight into the phase structure and dynamics of block copolymers is solid state NMR.^{27,30–32} The presence of various phases in an apparently homogeneous material can be easily verified by measuring proton relaxation times. The proton relaxation times both in the rotating frame ($T_{1\rho}(H)$) and in the laboratory frame ($T_1(H)$) are well known to be useful in elucidating the microphase structure on the nanometer scale, through the process called spin diffusion.^{30,33} Proton spin-lattice relaxation behavior can reflect the close relationships among the individual components, as indicated by proton spin-diffusion processes and measurements of the proton spin-lattice relaxation times for specific carbons in the copolymer, which support an analysis and identification of the microheterogeneous structures in terms of the differences in their relaxation behavior. The extent to which the averaging of relaxation times occurs depends on the degree of mixing and the relaxation times of the individual components. Additionally, these two proton relaxation times can provide insights into the heterophase domains on two size levels that differ by an order of magnitude, indicating this technique is appropriate to the study of the microstructure of copolymers. In the present study, a series of conducting urethane-aniline block copolymers were prepared and micro-

phase structures characterized by employing the solid state ^{13}C NMR combined with proton relaxation time measurements and TEM.

EXPERIMENTAL

Preparation of Amine-terminated Polyaniline Oligomer (OPA)

Aniline and ammonia persulfate (APS), mixed with 1 M HCl aqueous solution, were separately stored in a refrigerator overnight. A weight percent of 10 of *p*-phenylene diamine (*p*-PDA) was mixed with the aniline solution before APS aqueous solution was added dropwise into the aniline solution and the mixture was maintained at 0–5 °C for 24 h with continuous stirring. The resulting polyaniline was isolated by filtration and de-doped by stirring in a 0.1 M aqueous solution of ammonia for 12 h, followed by filtration. The cake was dried in a vacuum oven for three days and ground into powder using a mortar. The molar mass and molar mass distribution of the resulting OPA, were measured using a gel permeation chromatographer (GPC, Testhigh model 500) with mono-distributed polystyrene as the standard. The number average molecular weight and molecular weight distribution expressed as polydispersity index of the OPA were measured by gel permeation chromatograph and turned out to be 1380 and 1.69, respectively.

Preparation of PU-prepolymer

PU-prepolymer was prepared with a 2:1 mole ratio of purified 4-4'-diphenylmethane diisocyanate (MDI), which was purified by vacuum distillation, to poly(oxytetramethylene) glycol (PTMO) with a molecular weight of 1000 at 70 °C under nitrogen gas.

Preparation of PUU-OPA

OPA was dissolved in *N*-methyl pyrrolidone (NMP). The resulting PU-prepolymer in NMP was mixed with an equivalent amount of OPA-NMP mixture plus a chain extender (1,4-butanediol) at 70 °C until the isocyanate (-NCO groups) disappeared. The solution was then dried in a vacuum oven for three days. The molar ratio of the OPA to the chain extender was varied to control the content of the aniline-containing urethane-urea blocks in the copolymers but the total amount was kept equal to that of PUU-prepolymers. Samples were labeled according to the following notation: "PUU-OPA-x," where x refers to the OPA content in the copolymers.

^{13}C CP/MAS NMR

Solid-State ^{13}C cross-polarization (CP)/magic angle spinning (MAS) NMR experiments were conducted using a Bruker AVANCE-400 spectrometer, equip-

ped with a Bruker double-tuned 7 mm probe, with resonance frequencies of 100.6 MHz for ^{13}C nuclei and 400.1 MHz for ^1H nuclei. The Hartmann-Hahn condition for $^1\text{H} \rightarrow ^{13}\text{C}$ CP/MAS NMR experiments was determined using adamantane. Repetition times of 4 s were employed. ^{13}C CP/MAS NMR spectra were recorded using a CP contact time of 2 ms and at a spinning speed of 6.2 kHz. The ^{13}C chemical shifts were externally referenced to tetramethylsilane (TMS).

Proton Relaxation Time

$T_1(\text{H})$ relaxation times were indirectly measured by observing well-resolved ^{13}C resonances after application of the π - τ - $\pi/2$ (inversion-recovery) pulse sequence, followed by CP. The $T_{1\rho}(\text{H})$ relaxation times were determined by fitting the ^{13}C CP signal intensity as a function of contact time. The CP Hartmann-Hahn contact time was set to be 2 ms and a spin-locking field strength of 45 kHz was utilized. The proton decoupling field strength was 60 kHz was used in all experiments.

Conductivity

The Resistance (R) of the material was measured using a 4-probe measurement instrument and the conductivity was obtained from the formula

$$\sigma = L/(RA)$$

where L is thickness and A is cross-section area.

TEM

Transmission electron microscopy was undertaken using a JOEL TEM-200CX instrument at 120 KV. The TEM micro-photograph of PUU-OPA-x at a high magnification was obtained after the sprayed and dried sample was in embedded in the epoxy, cut into pieces around 70 nm long and the cross-sectioned were staining by exposing the sample to 1% ruthenium tetroxide (purchased from Aldrich Co.) vapor at 70 °C for two hours, and then dried at 50 °C under vacuum overnight by this procedure.

RESULTS AND DISCUSSION

^{13}C CP/MAS NMR Spectra of OPA and PU-prepolymer

The repeat unit of emeraldine base has been shown

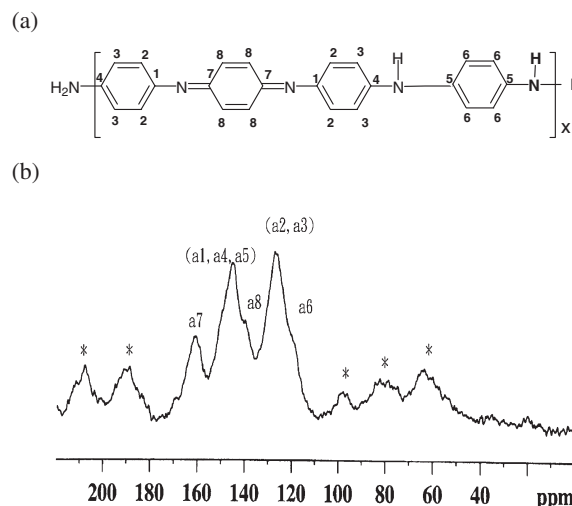


Figure 1. ^{13}C CP/MAS NMR spectrum of OPA (a) the emeraldine base form of polyaniline tetramer unit in the undoped state (b) the ^{13}C CP/MAS NMR spectrum of OPA along with carbons labeled. Asterisks denote spinning side bands.

by solid-state ^{13}C NMR to comprise a copolymer of reduced and oxidized bases in which two amine backbone nitrogens alternate with two imine backbone nitrogens (see Figure 1a).³⁴ Figure 1b presents the ^{13}C CP/MAS NMR spectrum of OPA. Broad resonances centered at around 124.1, 142.1, and 158.2 ppm are observed. The assignment of all different carbons, presented in Table I, consistent with a benzenoid-quinoid alternating structure, are those noted by Kaplan *et al.*³⁴ and Hjertberg *et al.*³⁵

Figure 2b displays the ^{13}C CP/MAS NMR spectrum of PU-prepolymer, Table II presented the observed ^{13}C chemical shifts. Those assignments are consistent with published results.³⁶ The peak observed in the carbonyl region at 154 ppm (Figure 2) are attributed to the urethane/urea carbonyl (C4) carbon. The aliphatic region is dominated by three carbon peaks at 27, 65 and 71 ppm that arise from the PTMO soft segment. The peak at 65 ppm is associated with soft-segment carbons that are next to a urethane link, whereas the peak at 27 ppm is attributed to those PTMO soft-segment internal CH_2 carbons (C3); the peak at 71 ppm is corresponds to those PTMO soft-segment external CH_2 carbons (C2). The smaller peak at 40 ppm corresponds to the methylene carbon (C5) in the MDI hard segment. The five different primary

Table I. The observed ^{13}C chemical shifts and peak assignments of OPA

Sample*	Benzenoid protonated ring	Quinoid protonated ring	Benzenoid quaternary ring	Quinoid quaternary ring
PANI ³⁵	124.5	137.5/142	148	158
OPA	124.1	142.1	146.7	158.2

*Both in emeraldine base form.

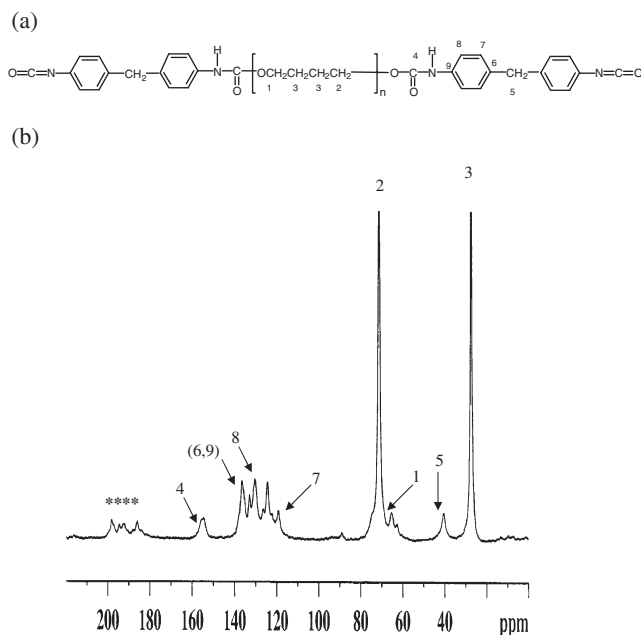


Figure 2. ^{13}C CP/MAS NMR spectra of PU-prepolymer (a) The repeat unit of PU-prepolymer and (b) the ^{13}C CP/MAS NMR spectrum of PU-prepolymer along with carbons labeled. Asterisks denote spinning sidebands.

Table II. The observed ^{13}C chemical shifts and peak assignments of PU-prepolymer

Assignment (carbon no.)	Chemical shift, ppm
PTMO internal CH_2 (C3)	27
PTMO external CH_2 (C2)	71
MDI CH_2 (C5)	40
PTMO CH_2 adjacent to urethane (C1)	65
MDI protonated ring (C7)	119
MDI protonated ring (C8)	129
MDI quaternary ring (C6/C9)	136
MDI urethane/urea carbonyl (C4)	154

peaks ranging from 115 to 140 ppm can be assigned to aromatic carbons. The peak at 136 ppm is assigned to the quaternary MDI ring carbons (C6, C9), and the peaks at 119 and 129 ppm are assigned to the protonated aromatic MDI carbons (C7, C8). The peaks at 125 and 133 ppm may result from conformational differences in the solid state, as indicated by dipolar dephasing experiments.³⁶

^{13}C CP/MAS NMR Spectra of PUU-OPA

Figure 3 shows the ^{13}C CP/MAS spectra of PUU-OPA-x for various OPA contents. The OPA carbons and the aromatic rings of the PU-prepolymer all contribute to the aromatic region. The ^{13}C CP/MAS NMR spectrum of the PUU-OPA-0.1 is merely a superposition of the individual spectra of the component polymers. OPA and PU-prepolymer, except in that the

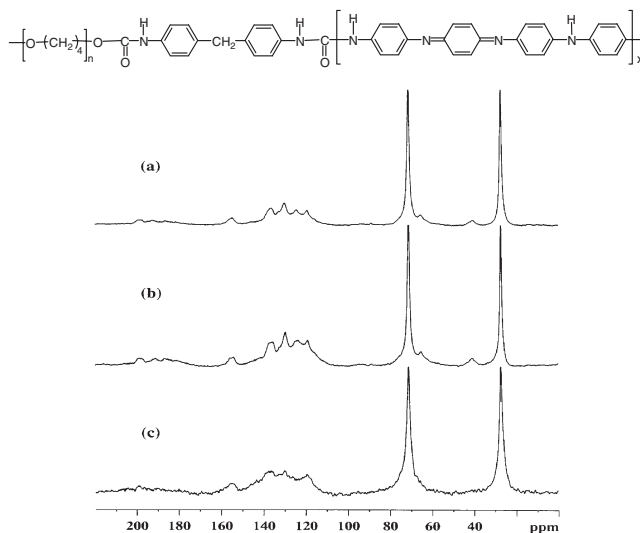


Figure 3. ^{13}C CP/MAS NMR spectra of PUU-OPA-x sample (a) $x = 0.1$, (b) $x = 0.2$, (c) $x = 0.3$.

methylene peak of MDI at 40 ppm became broader as the OPA was copolymerized with PU-prepolymer. The decline in the intensity of CH_2 of MDI as the content of OPA is increased, is related to the CH_2 groups that are bound adjacent bound to the OPA block. Generally, distinct changes in the ^{13}C CP/MAS NMR spectrum of a given copolymer depend on some interaction over a distance comparable to that of a few bonds, ~ 1 nm or less, such that the electron clouds of individual components are disturbed. Although some chemical bonds are present at the conjunction points between PUU and OPA block, the interaction strength is too small to cause changes in chemical shifts and line shapes in the soft segment peaks in the ^{13}C CP/MAS NMR spectrum with the increase in the content of OPA. Notably, the peaks at 125 and 133 ppm become less well resolved as OPA is added, revealing that the copolymerization of OPA with PUU alters the conformation of the PUU-prepolymer in the solid state. The line width in the aromatic region gradually increase with the content of OPA, because of the extended overlap between OPA and PU-prepolymer (*cf.* Table I and II). Therefore, this work focus only on the change in proton relaxation times, to provide information about the sizes of the domains, formed by the soft segment in the copolymers studied herein.

Contact Time and Proton Relaxation Time Measurements

Proton spins are abundant, so the spin-lattice relaxation times $T_1(\text{H})$ and $T_{1\rho}(\text{H})$ of polymers can be considered to investigate the phase structure in polymers. Measurements of proton spin-lattice times in both the laboratory frame ($T_1(\text{H})$) and in the rotating frame

Table III. $T_1(\text{H})$ of PUU-OPA- x sample ($x = 0, 0.1, 0.2$ and 0.3) and the spin-diffusion path lengths

Chemical shift, ppm	$T_1(\text{H}), \text{s}$			
	PUU-OPA- x			
	$x = 0$	0.1	0.2	0.3
27	0.51 ± 0.02	0.51 ± 0.05	0.55 ± 0.05	0.55 ± 0.05
71	0.50 ± 0.04	0.50 ± 0.05	0.53 ± 0.05	0.55 ± 0.05
Spin-diffusion path length, nm	43.2	43.3	45.1	45.2

($T_{1\rho}(\text{H})$) were made for the block copolymer samples, and compared with those of the PUU-prepolymer.

In the $T_1(\text{H})$ experiment, the inversion recovery approach was applied, and the resonance intensities were measured as functions of delay time. Table III lists the measured $T_1(\text{H})$ relaxation results. The $T_1(\text{H})$ values of PUU in the block copolymers differ slightly from those of the PU-prepolymer, revealing that OPA block mixing PUU must have taken place. The spin-diffusion path length of PUU ranges from 43.2 to 45.2 nm. For PUU-OPA- x copolymers, the proton T_1 relaxation times of various carbons in the block copolymer are identical to within 10% experimental uncertainty, indicating that the spin diffusion process across the mixed domain of PUU and OPA is fast enough to average out the T_1 values of the individual protons. The T_1 value indicates magnetic homogeneity at that level within the sample.

In order to gain more insight into the influence of the content of OPA on the microstructure of PUU-OPA- x copolymers, $^1\text{H} \rightarrow ^{13}\text{C}$ CP/MAS NMR experiments have been performed as a function of contact time, ranging from 0.1 to 20 ms. Theoretically, the intensity of ^{13}C CP signals is expected to increase with increasing contact time until the transfer of magnetization is optimal, then the signal should decay due to the rotating frame relaxation. The dependence of peak intensity, $M(t)$, on contact time can be expressed by the following formula:³⁷

$$M(t) = M_0 \exp(-t/T_{1\rho}(\text{H})) (1 - \exp(-t/T_{\text{CH}})) \quad (1)$$

where M_0 is the normalization constant, $T_{1\rho}(\text{H})$ represents the proton spin-lattice relaxation time in the rotating frame, and T_{CH} is the cross-polarization constant. Table IV lists the contact time measurements that corresponds to the soft segment carbon peaks. Table IV shows a gradual decrease for T_{CH} of the soft segment carbons as the content of OPA is increased. The T_{CH} of 27 ppm ranges from 808.3 μs to 109.6 μs , and T_{CH} of 71 ppm ranges from 421.7 μs to 96.5 μs . The efficiency of CP transfer depends inversely on mobility, so a decrease in T_{CH} values reflects an increase in the chain rigidity of the soft segments, probably caused by the inter-chain interactions be-

Table IV. T_{CH} and $T_{1\rho}(\text{H})$ of the soft segment carbons in the PUU-OPA- x samples ($x = 0, 0.1, 0.2, \text{ and } 0.3$) and the corresponding spin-diffusion path lengths

Chemical shift, ppm	x	$T_{\text{CH}}, \mu\text{s}$	$T_{1\rho}(\text{H}), \text{ms}$	Spin-diffusion path length, nm
27	0	808.3	52.4	9.9
	0.1	693.3	35.1	8.1
	0.2	814.6	33.7	7.9
	0.3	109.6	10.9	4.5
71	0	421.7	20.0	6.1
	0.1	439.6	15.7	5.4
	0.2	465.3	15.4	5.3
	0.3	96.5	5.8	3.3

tween $-\text{NH}$ in the OPA unit and the ether oxygen atoms. Because of the poor sensitivity in the carbonyl region for the urethane/urea (154 ppm, C4) carbon, it is difficult to accurately analyze their respective relaxation times.

Unlike the $T_1(\text{H})$ values, the $T_{1\rho}(\text{H})$ values obtained from individual chemical positions in a copolymer differ. This observation indicates that distinct proton spin reservoirs are coupled to the various carbons, revealing proton-proton spin diffusion is relatively slow because of the phase separation in PUU-prepolymer. The $T_{1\rho}(\text{H})$ values for the protons associated with the soft segment increases slightly for PUU-OPA-0.1, but decreases at the higher content of OPA. $T_{1\rho}(\text{H})$ values are determined mainly by the dipolar interaction, which depends on the amplitude and frequency of the motion of protons and depends inversely on the proton-proton distances. If proton densities of the hard and soft phases are assumed to be invariant with the increase of the content of OPA, then change in $T_{1\rho}(\text{H})$'s values exhibited by both phases are caused by motional changes. This observation suggests that the possible inter-chain interactions between OPA and the soft segments in the polymer chains effectively reduce the chain mobility, resulting in the increase in the chain rigidity, and therefore increases proton-proton dipolar interaction.

Estimated Phase Size

If ^1H NMR magnetization of the whole sample reaches equilibrium within the relaxation times of individual and separated phases, then even the materials and the systems comprising more than one phase will exhibit the same relaxation time. The $T_1(\text{H})$ values of the PUU-OPA- x samples ($x = 0, 0.1, 0.2$ and 0.3) are in the range of 0.4 to 0.6 s. Table III shows that all signals associated with the soft segment of the PUU yield the same $T_1(\text{H})$ values when the experimental error is considered. Like $T_1(\text{H})$ relaxation times, if a given block copolymer is completely molecularly

Table V. Dependence of Conductivity of PUU-OPA doped with 1.0 M HCl on OPA composition

Physical property	PUU-OPA-x				
	x = 0	0.1	0.2	0.3	1.0
Conductivity (S/cm)	—	$(1.96 \pm 0.01) \times 10^{-6}$	$(1.52 \pm 0.02) \times 10^{-5}$	$(6.62 \pm 0.03) \times 10^{-4}$	$(8.3 \pm 0.03) \times 10^{-1}$

homogenous (on the scale of around a few nanometers or less), then the $T_{1\rho}(\text{H})$ values of the component polymers in the block copolymer must be the same. However, the $T_{1\rho}(\text{H})$ values associated with the various soft segment carbons in the PUU-OPA copolymers are quite different. Hence, the equilibration time of ^1H NMR magnetization for each PUU-OPA sample must lie between the $T_{1\rho}(\text{H})$ and the $T_1(\text{H})$ values. The spin equilibration time depends on the domain size and the spin diffusion coefficients of various phases. The minimum size level that can be obtained from the spin-lattice relaxation times can be estimated by the following equation:³⁸

$$\langle L \rangle = (6DT)^{1/2} \quad (2)$$

where L is the spin-diffusion path length (*i.e.*, the domain size) in time T (which here must be equated with the spin-lattice relaxation time, $T_1(\text{H})$ or $T_{1\rho}(\text{H})$) and D is the spin diffusion coefficient determined by the mean proton-proton distance and the strength of the dipolar interaction; it is of the order of $4\text{--}7 \times 10^{-16} \text{ m}^2 \text{ s}^{-1}$ for a rigid proton system.^{39,40} The minimum size of phase can be determined from the spin diffusion coefficient of the PUU, which is unavailable. As an approximation, the spin diffusion coefficient of alkane ($6.2 \times 10^{-16} \text{ m}^2/\text{s}$)³⁹ can be used here as a substitute for the unknown PU diffusion coefficient. Table III shows the spin-diffusion path length, obtained from the $T_1(\text{H})$ relaxation times, of PUU-OPA copolymers, which is estimated to be around 40–50 nm, so the PUU-OPA-x samples are homogeneous on this scale. The maximum diffusive path length, L , obtained from $T_{1\rho}(\text{H})$, often reflects the minimum size of the microdomain. Table IV presents the T_{CH} and $T_{1\rho}$ values of the soft segment carbons in the PUU-OPA-x copolymers and the corresponding spin-diffusion path length. Based on the largest $T_{1\rho}(\text{H})$ value, which is 35.1 ms, obtained from the 27 ppm (C3) of the PUU-OPA-0.1 sample, the maximum diffusive path length is estimated to be around 8.1 nm, by considering the fact that in the rotating frame the spin diffusion coefficient D is scaled by a factor of $1/2$.⁴⁰ The actual soft segment phase size (dispersed phase size) should exceed the spin-diffusion path length during $T_{1\rho}(\text{H})$ and be smaller than it during $T_1(\text{H})$ because the relaxation times in the rotating frame vary only one is observed in the laboratory. Therefore, the minimum domain size of the

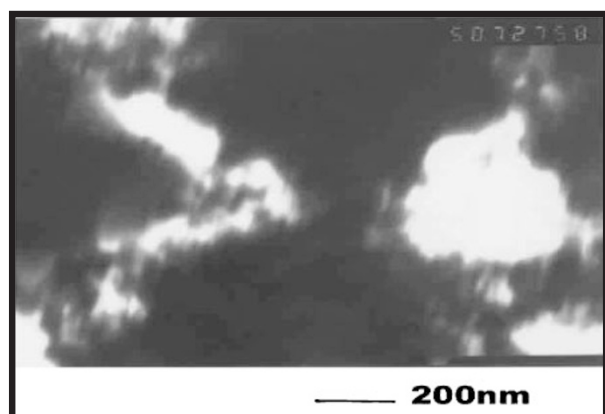
soft segments in the PUU-OPA-0.1 samples is around 8.1 nm. Unfortunately, the domain sizes of the OPA and the hard segments can not be estimated because the extended overlap of the signals in the aromatic regions and the severe peak broadening of the 40 ppm carbon in the hard segment prevents the determination of relaxation times in these regions.

Conductivity

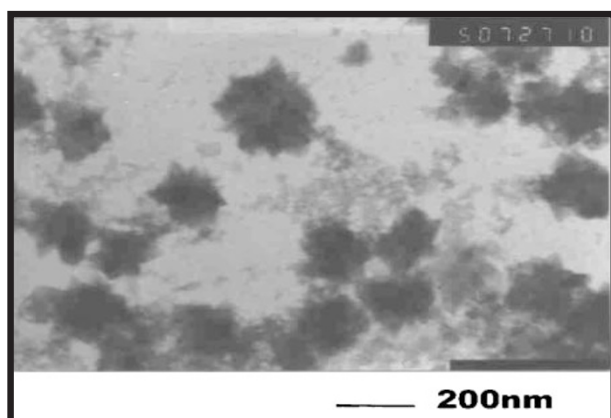
Table V presents the dependence of the electronic conductivity of the aniline-containing copolymers on aniline content. It ranges from 0.83 S/cm for the polyaniline oligomer (OPA) to $1.96 \times 10^{-6} \text{ S/cm}$ for the PUU-OPA doped with 1.0 M HCl. The conductivity of the urethane-aniline block copolymers doped with 1.0 M HCl is less than that of the neat OPA doped with the same concentration of HCl, because the conductive OPA blocks in the copolymer are prepared and diluted in the matrix, such that electron transfer is more restricted than that in the neat OPA. The conductivity of the block copolymers increases with aniline content in the copolymer because the aniline-oligomer blocks were distributed randomly and in contacted with each other, because the interactions among the blocks were facilitating the transportation or jumping of electrons from one end of the aniline-oligomer block to another. The conductive aniline-containing blocks (the hard segments) may come into contact with each other, forming a continuous conductive bridge even though the electron transfer is restricted by the polyurethane *via* the chemical bonding in the structure.

TEM Results

Figure 4 displays TEM photographs of PUU-OPA with various OPA contents. Microscopic investigation of solvent-cast films indicates that small black spots which dominate in OPA (hard-segment domain of size 60–300 nm) are scattered in a matrix that is rich in PTMO (soft-segment domain). Hence, the conducting copolymers undergo microphase separation. The distribution of hard-segment domains (richer in OPA) is scattered and these domains connected into the network structure in copolymers, that contain 30% OPA. The connected conductive network structure can form a continuous and effective conducting bridge in copolymers.



(a)



(b)

Figure 4. Transmission electron micrographs of PUU-OPA-x sample (a) $x = 0$, (b) $x = 0.3$ (1 cm = 200 nm).

CONCLUSIONS

The introduction of aniline-oligomer blocks as a chain extender into the polyurethane backbone can significantly affect the properties of the resultant urethane-aniline block copolymers through the copolymerization between the urethane blocks and aniline-oligomer urea blocks. The conductivity of the copolymers are rise sharply with the aniline content of the copolymers. It ranges from 1.96×10^{-6} S/cm to 0.83 S/cm. TEM and ^{13}C NMR analysis revealed the separated microphases. Proton T_1 data indicate that PUU-OPA-x copolymer is homogeneous on a scale of greater than around 40–50 nm. Various contact time CP experiments established that T_{CH} and $T_{1\rho}(\text{H})$ of the soft segment carbons decrease as the content of OPA increased. These results indicate that the chain mobility and the domain size of the soft segment decline as the content of OPA increases. The $T_{1\rho}(\text{H})$ data reveal that the minimum domain size of the studied PUU-OPA-x samples is estimated to be around 8.1 nm.

Acknowledgment. The authors would like to thank the National Science Council of Taiwan, R. O. C., under Contract No. 92-2216-E-224-003. The authors thank Dr. H. M. Kao for her help with the NMR measurement, as well as the R.R. Wu Fellowship.

REFERENCES

1. A. G. MacDiarmid and A. J. Epstein, *Faraday Discuss.*, **88**, 317 (1989).
2. M. Kaneko and H. Nakamura, *J. Chem. Soc. Chem. Commun.*, 1441 (1985).
3. A. G. MacDiarmid, J. C. Chang, A. F. Richter, NLD Somasiri, and A. J. Epstein, in "Conducting Polymers," L. Alcacer, Ed., Reidel Publishing Co. Holland, 1987, p 105.
4. C. Y. Yang, Y. Cao, P. Smith, and A. J. Heeger, *Synth. Met.*, **53**, 823 (1993).
5. Y. Cao, P. Smith, and A. J. Heeger, *Synth. Met.*, **32**, 263 (1989).
6. Y. Cao, P. Smith, and A. J. Heeger, *Synth. Met.*, **48**, 91 (1992).
7. Y. Cao, A. Andreatta, A. J. Heeger, and P. Smith, *Polymer*, **30**, 2305 (1989).
8. J. Y. Lee, D. Y. Kim, and C. Y. Kim, *Synth. Met.*, **74**, 103 (1995).
9. J. Y. Lee, K. T. Song, S. Y. Kim, D. Y. Kim, and C. Y. Kim, *Synth. Met.*, **84**, 137 (1997).
10. K. T. Song, J. Y. Lee, H. D. Kim, D. Y. Kim, S. Y. Kim, and C. Y. Kim, *Synth. Met.*, **110**, 57 (2000).
11. J. W. Chevalier, J. Y. Bergeron, and L. H. Bao, *Polym. Commun.*, **30**, 308 (1989).
12. L. W. Shacklette, J. F. Wolf, S. Gould, and R. H. Baughman, *J. Chem. Phys.*, **88**, 3955 (1988).
13. Y. Wei, C. Yang, G. Wei, and G. Feng, *Synth. Met.*, **84**, 289 (1997).
14. Y. Cao, S. Z. Li, Z. J. Xue, and D. Guo, *Synth. Met.*, **16**, 305 (1986).
15. E. M. Conwell, C. B. Duke, A. Paton, and S. Jeyadev, *J. Chem. Phys.*, **88**, 3331 (1988).
16. F. L. Lu, F. Wudl, M. Nowak, and A. J. Heeger, *J. Am. Chem. Soc.*, **108**, 8311 (1986).
17. Y. Wei, C. Yang, and T. Ding, *Tetrahedron Lett.*, **37**, 731 (1996).
18. Y. Wei, C. Yang, T. Ding, J. M. Yeh, and G. Wei, *Polym. Mater. Sci. Eng.*, **74**, 209 (1996).
19. L. M. Leung and J. T. Koberstein, *J. Polym. Sci. Polym. Phys. Ed.*, **23**, 1883 (1985).
20. J. T. Koberstein and L. M. Leung, *Macromolecules*, **25**, 6205 (1992).
21. G. Bidan, E. M. Genies, and J. F. Penneau, *Electronal. Chem.*, **271**, 59 (1989).
22. S. Dong and Z. Li, *Synth. Met.*, **33**, 93 (1989).
23. A. Watanabe, K. Mori, and A. Iwabuchi, *Macromolecules*, **22**, 3521 (1989).
24. Y. Wei, R. Hariharid, and S. A. Patel, *Macromolecules*, **23**, 758 (1990).
25. D. Kumar, *Synth. Met.*, **114**, 369 (2000).
26. J. Y. Liu, C. C. Yang, and Y. Z. Wang, *J. Appl. Polym. Sci.* (revised) (2005).

27. T. Fujiwara and K. J. Wynne, *Macromolecules*, **37**, 8491 (2004).
28. T. M. Alam, B. R. Cherry, K. R. Minard, and M. Celina, *Macromolecules*, **38**, 10694 (2005).
29. V. D. S. Martijn, V. D. H. Evert, F. Jan, and J. G. Reinoud, *Polymer*, **46**, 3616 (2005).
30. P. Peyser, in "Polymer Handbook," 3rd ed., J. Brandrup and E. H. Immergut, Ed., Wiley Interscience, New York, N.Y., 1989.
31. E. Murray and D. F. Broughamb, *Synth. Met.*, **155**, 681 (2005).
32. Y. Yang and W. Yang, *Polym. Adv. Technol.*, **16**, 24 (2005).
33. H. Tanaka and T. Nishi, *Phys. Rev. B: Condens. Matter Mater. Phys.*, **33**, 32 (1986).
34. S. Kaplan, E. M. Conwell, A. F. Richter, and A. G. MacDiarmid, *J. Am. Chem. Soc.*, **110**, 7647 (1988).
35. T. Hjertberg, W. R. Salaneck, I. Lundstrom, N. D. Somasiri, and A. G. MacDiarmid, *J. Polym. Sci., Polym. Lett.*, **23**, 503 (1985).
36. D. T. Okamoto, S. L. Cooper, and T. W. Root, *Macromolecules*, **25**, 1068 (1992).
37. M. Mehring, "Principle of High-Resolution NMR in Solids," 2nd ed., Springer-Verlag, New York, 1983.
38. J. R. Havens and D. L. VanderHart, *Macromolecules*, **18**, 1663 (1985).
39. D. C. Douglass and G. P. Jones, *J. Chem. Phys.*, **45**, 956 (1966).
40. J. Clauss, K. Schmidt-Rohr, and H. W. Spiess, *Acta Polym.*, **44**, 1 (1993).